

Article

Catalytic Activity of Carbon Materials in the Oxidation of Minerals

Aura Alejandra Burbano ¹, Gabriel Gascó ², Jorge Paz-Ferreiro ³  and Ana Méndez ^{4,*} 

¹ INQUISUR, Departamento de Química, Universidad Nacional del Sur (UNS)-CONICET, Av. Alem 1253, Bahía Blanca 8000, Argentina

² Department of Agricultural Production, Universidad Politécnica de Madrid, Ciudad Universitaria, 28040 Madrid, Spain

³ School of Engineering, RMIT University, Melbourne, VIC 3001, Australia

⁴ Department of Geological and Mining Engineering, Universidad Politécnica de Madrid, 28040 Madrid, Spain

* Correspondence: anamaria.mendez@upm.es

Abstract: This study aims to advance the knowledge of using carbon materials as catalysts in the oxidation of chalcopyrite. For this, two different materials (a commercial activated carbon (CC) and commercial biochar (BC)) were added to chalcopyrite ore (CPY) at three weight ratios (1:1, 1:0.5, and 1:0.25). Mixtures were treated with sulfuric/ferric solution for 96 h at 90 °C. Experimental results showed that extraction of copper from CPY was around 36%, increasing to higher than 90% with the addition of CC or BC at the proper ratio. The best result (99.1% Cu extraction) was obtained using a 1:1 ratio of CPY:CC. Analysis of solid residues shows that CC, with a high surface area, adsorbs sulfur onto its surface, limiting elemental sulfur formation. Additionally, the treatment of CPY in the CC's presence transforms the chalcopyrite into CuS. Sulfur adsorption or CuS formation was not observed after the leaching of chalcopyrite with BC. However, the addition of BC to CPY at a ratio of 1:0.25 also increased the extraction of copper to 91.1%. Two carbon materials were oxidized after treatment with a sulfuric/ferric solution, and BC probably displayed catalytic properties in the leaching medium.

Keywords: biochar; activated carbon; catalyst; chalcopyrite; oxidation



Citation: Burbano, A.A.; Gascó, G.; Paz-Ferreiro, J.; Méndez, A. Catalytic Activity of Carbon Materials in the Oxidation of Minerals. *Catalysts* **2022**, *12*, 918. <https://doi.org/10.3390/catal12080918>

Academic Editor: David Sebastián

Received: 14 July 2022

Accepted: 16 August 2022

Published: 19 August 2022

Publisher's Note: MDPI stays neutral with regard to jurisdictional claims in published maps and institutional affiliations.



Copyright: © 2022 by the authors. Licensee MDPI, Basel, Switzerland. This article is an open access article distributed under the terms and conditions of the Creative Commons Attribution (CC BY) license (<https://creativecommons.org/licenses/by/4.0/>).

1. Introduction

The increasing need for materials for various important applications, a growing world population, and the fact that our Earth's resources are limited raise the question of future material supply. Several industry activities, policy initiatives, and research projects have recently been initiated in Europe with the aim to ensure an adequate supply of raw materials [1]. Copper, the third metal by global production volume after iron and aluminum, is an essential material for emerging technologies such as electric cars, photovoltaic panels, and wind generators, which will increase copper demand [2,3]. The depletion of world reserves of high-grade minerals is causing an increase in the price of copper and, consequently, exploitation of lower-grade deposits. Unfortunately, increasing copper extraction and decreasing ore grades intensify energy use and generate a higher environmental impact, leading to the need to develop advanced mining and metallurgical technologies with lower environmental impacts [4].

Chalcopyrite, the resource with the highest copper content, represents about 70–80% of known world copper reserves [5–7]. Similar to other copper sulfides, this mineral is usually exploited in deposits with grades as low as 0.4–0.5% copper. The exploitation of these reserves is within the limits of economic viability using traditional pyrometallurgical treatment of sulfide concentrates. However, chalcopyrite is refractory in acid media, with low dissolution rates that hinder the hydrometallurgical route. This refractoriness is attributed to the formation of passive layers of elemental sulfur [8–11], copper-rich polysulfides [12,13], or iron salts [14,15] on the chalcopyrite surface particles. These coating layers have low electrical conductivity and can prevent the transfer of electrons and ions to the core of chalcopyrite, hindering copper extraction [16].

The addition of several species to improve the extraction of copper from chalcopyrite in acidic sulfuric media has been investigated. For example, the addition of pyrite [17,18] NaCl [19], manganese dioxide [20,21], nano-silica [22], and carbon materials [20,23,24] have demonstrated their capacity to increase the copper leaching. Nakazawa [23] concluded that the improved kinetics of chalcopyrite leaching could be due to two factors: (1) decrease in the redox potential and (2) galvanic interaction between carbonaceous structures and chalcopyrite. Alvarez et al. [25] studied the effects of different carbon materials on the leaching of copper and zinc from a complex sulfide mineral—rich in chalcopyrite, pyrite, and sphalerite. They concluded that the added carbon materials reduced the Eh of the leaching systems, but not all of them improved copper extraction. Despite the advances in recent years, there is a lack of knowledge about the mechanism involved in the leaching of sulfide minerals in the presence of carbon materials, as carbon materials with different properties can act as catalysts [23–25]. Thus, the main objective of this research is to advance the knowledge of using carbon materials as potential catalysts in the oxidation of sulfide minerals in sulfuric/ferric solutions. For this research, two commercial carbon materials with different properties (CC and BC) were added to selected chalcopyrite ore (CPY) in three different ratios. An exhaustive characterization of the feedstocks and final solid residues was performed by XRD and SEM-EDS analysis. Additionally, CC and BC were treated with sulfuric/ferric solutions for 48 h at 90 °C in order to assess the interaction between the leaching agent and the carbon materials and to identify possible modifications to carbonaceous structures during the leaching process.

2. Results

2.1. Feedstock Characteristics

The chemical composition, pH, and Eh of the CPY are summarized in Table 1.

Table 1. pH, Eh, and elemental composition of CPY sample.

Element	Value
Fe	32.9 ± 0.2 wt%
Cu	28.3 ± 0.2 wt%
S	15.5 ± 0.2 wt%
Mg	1.4 ± 0.1 wt%
Al	1.2 ± 0.1 wt%
Si	1.0 ± 0.1 wt%
Ca	0.84 ± 0.04 wt%
Zn	0.21 ± 0.01 wt%
As	0.14 ± 0.01 wt%
Co	0.09 ± 0.01 wt%
pH	3.96 ± 0.2
Eh	436 ± 3.0 mV

The main elements present in the CPY were Fe (32.9%), Cu (28.3%), and S (15.5%), with small amounts of Mg (1.4%), Al (1.2%), Si (1.0%), Ca (0.8%), and Zn (0.2%). Also, it is important to note the presence of Co in the ore sample. The XRD analysis of CPY (Figure 1) showed that the main mineralogical species were chalcopyrite (58.1%) and pyrite (34.2%), with small amounts of siderite (7.5%) and sphalerite (0.2%).

Figure 2 shows the N₂ adsorption–desorption isotherms of CC (Figure 2a) and BC (Figure 2b). The adsorption of N₂ at low relative pressure ($p/p_0 < 0.1$) of CC is related to microporosity, while the BC isotherm was related to the presence of mesoporosity in its structure. The hysteresis loops showed the existence of some capillary condensation.

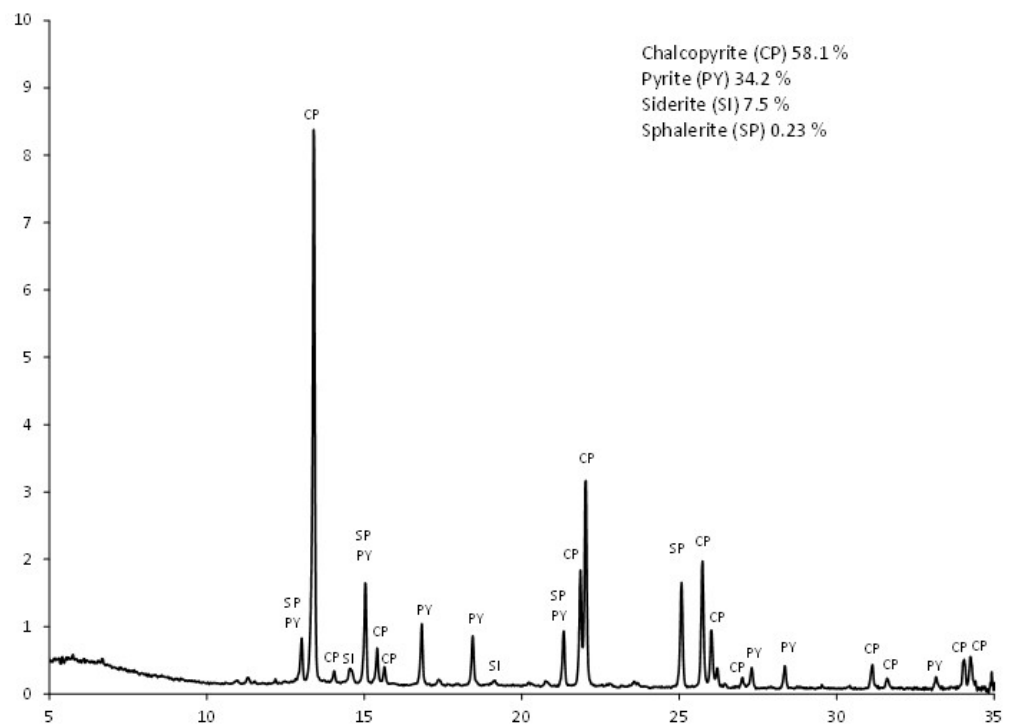


Figure 1. XRD pattern of CPY sample.

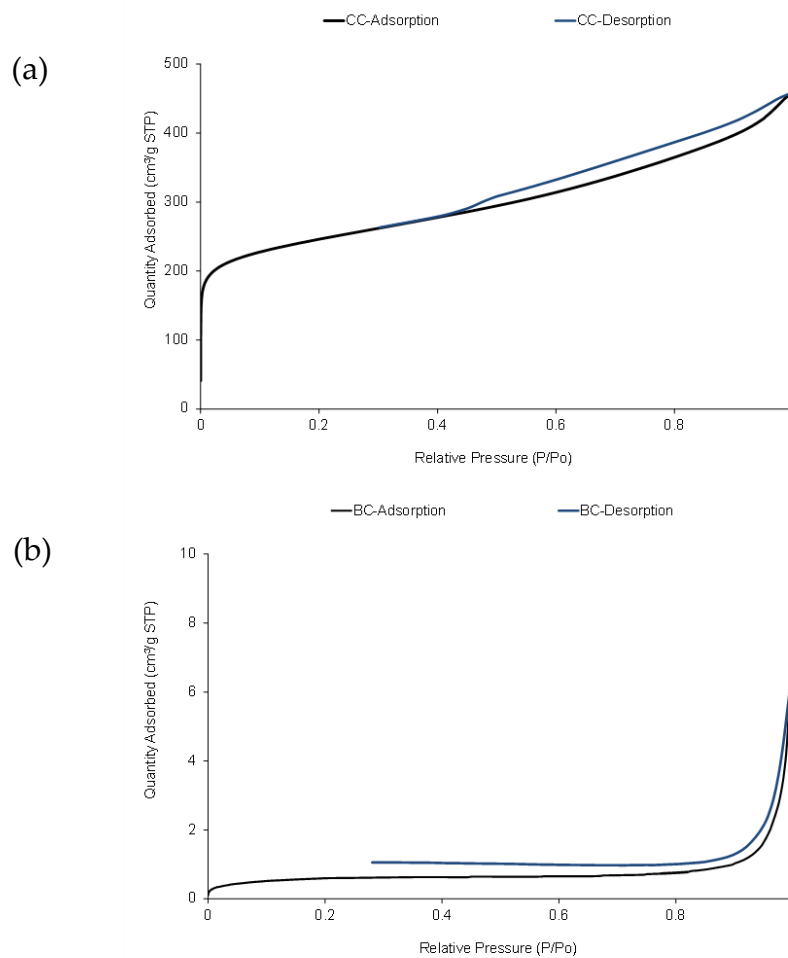


Figure 2. N₂ isotherms of (a) CC and (b) BC carbon materials.

The two carbon materials (CC and BC) showed different oxygen content (Table 2), which was higher for the CC material (12.39%). Carbon content was also higher in CC (85.72%) than in BC (80.21%). The H/C, O/C, and (O+N)/C ratios were calculated considering the contents of C, H, O, and N in the samples. CC had a lower H/C ratio (0.12), indicating higher aromaticity than BC (H/C ratio of 0.47). FTIR analysis of both samples was carried out to broaden the characterization of the oxygenated functional groups of the carbon materials (Figure 3). The main differences were observed in the relative intensity of the bands. The broad band at 3400 cm^{-1} is attributed to $-\text{OH}$ stretching vibration in the carboxyl and hydroxyl groups. This peak exhibited more intensity in CC material. The small bands at 2900 and 2850 cm^{-1} indicate that both materials had a low content of aliphatic structures.

Table 2. Main properties of carbon materials (CC and BC) and carbon materials after treatment with leaching solution (CCt and BCt).

Sample	Ash Content (%)	C (%)	H (%)	N (%)	S (%)	O (%)	H/C	O/C
CC	1.00	85.72	0.88	0.00	0.00	12.39	0.12	0.11
BC	14.94	80.21	3.12	0.92	0.00	0.81	0.47	0.01
CCt	0.29	78.90	1.53	0.00	0.41	18.87	0.23	0.18
BCt	0.86	75.38	3.17	0.52	0.11	19.98	0.51	0.20

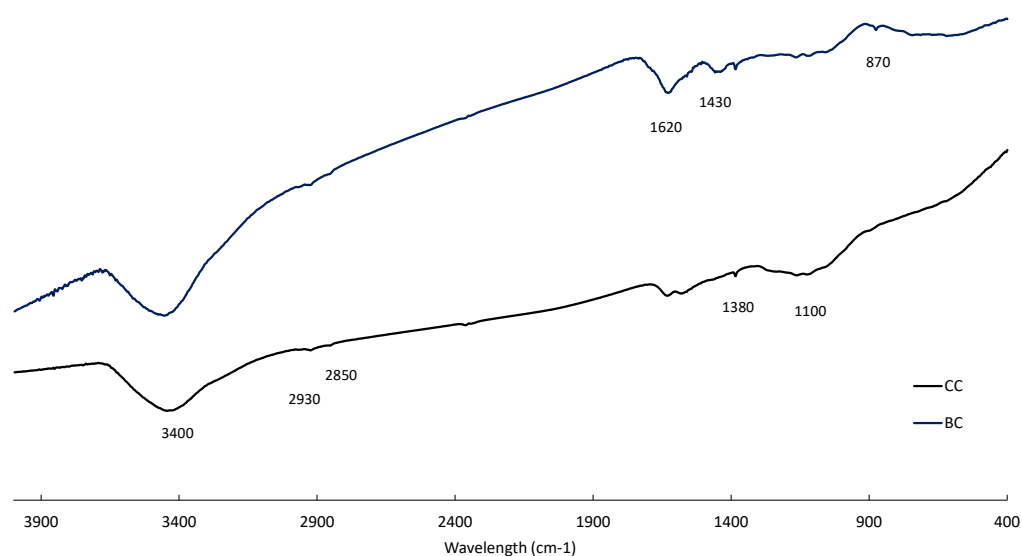


Figure 3. FTIR spectra of carbon materials: CC and BC.

This result was expected and in agreement with the low values of the H/C molar ratios (Table 3). The band at 1620 cm^{-1} can be attributed to $\text{C}=\text{O}$ vibrations in carboxylic acids, esters, lactones, and quinones becoming more intense in CC than in BC, probably due to the formation of oxygen functional groups during the activation process of commercial activated carbon (CC). The band at 1450 cm^{-1} is related to $\text{C}=\text{C}$ stretching in aromatic structures, whereas the small peak at 870 cm^{-1} is associated with $\text{C}-\text{H}$ aromatic groups. The intensity in these two areas was higher for CC material, according to their lower H/C molar ratio (Table 3). The small bands at 1580 cm^{-1} could be related to $\text{N}-\text{H}$ in amines and amides. Their intensity is higher in BC, agreeing with that material's higher N content (Table 3). The small band at 1380 cm^{-1} can be attributed to $\text{C}-\text{O}$ in ether and phenolic groups or to the existence of $\text{C}-\text{N}$ groups. Finally, the broad band from $1000\text{--}1300\text{ cm}^{-1}$ is related to the presence of stretching of aliphatic ethers ($\text{C}-\text{O}-\text{C}$) and alcohols ($\text{C}-\text{O}$). Moreover, $\text{Si}-\text{O}$ stretching related to the presence of SiO_2 can be observed in this region. Its intensity was higher for the BC material because of its higher ash content.

Table 3. Total extraction of Cu (%) after leaching process at 90 °C for 96 h.

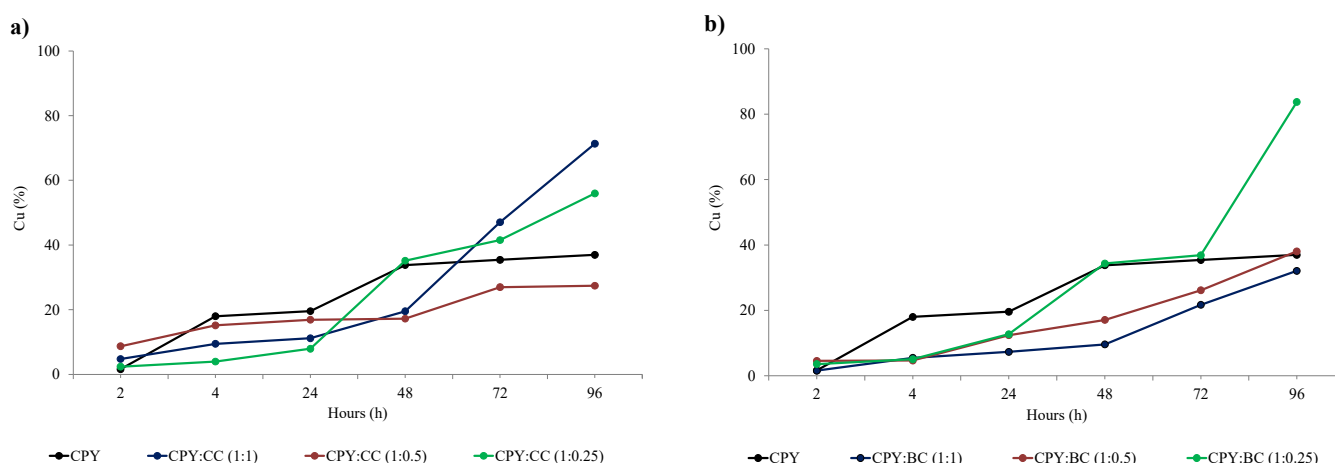
Sample	Total Cu (%)
CPY	37.0 ± 1.6
CPY:BC (1:1)	32.1 ± 1.5
CPY:BC (1:0.5)	53.5 ± 2.5
CPY:BC (1:0.25)	91.1 ± 3.0
CPY:CC (1:1)	99.1 ± 2.0
CPY:CC (1:0.5)	51.3 ± 2.7
CPY:CC (1:0.25)	56.0 ± 2.3

2.2. Total Copper Extraction after the Leaching Process

Table 3 shows the total copper extraction from CPY after 96 h of the leaching process. The total copper extracted from CPY, without carbon addition, was 36.98%. This value is similar to the results of previous studies [7,26] according to the refractoriness of chalcopyrite and lower than that obtained in the leaching of complex sulfide minerals (63%) [25]. The addition of CC increased copper extraction by more than 51.34%, and it reached 99.1% for the CPY:CC 1:1 ratio. Furthermore, the addition of BC increased copper extraction from 53.5% (ratio 1:0.5) to 91.1% (ratio 1:0.25).

2.3. Evolution of Copper Extraction during Leaching Experiments

Figure 4 shows the evolution of copper extraction (%) over time.

**Figure 4.** Evolution of copper extraction in the leaching solution: (a) CC and (b) BC.

2.4. FTIR Analysis of CC and BC after Treatment with Leaching Solution

Figure 5 shows the FTIR of CC and BC after sulfuric/ Fe^{3+} treatment. Compared to Figure 3, treatment with a leaching agent changed the surface chemical composition of CC and BC. Treated BC showed more intensity of the bands at 1630 and 1380 cm^{-1} related to C=O groups such as carboxylic acids and quinones and C-O in the ether and phenolic groups. Finally, according to the increase in H/C (Table 1), treated BC and CC showed a high intensity of bands at 2930 and 2850 cm^{-1} .

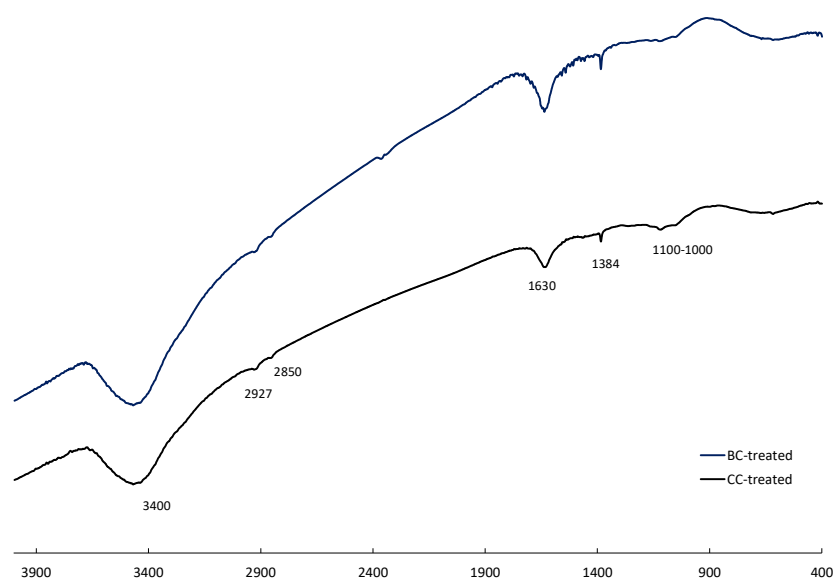


Figure 5. FTIR spectra of carbon materials after treatment with leaching solution (CCt and BCt).

2.5. Eh Evolution during Leaching Experiments

Figure 6 shows the evolution of Eh during leaching experiments. Eh decreased after the first 2 h of CPY extraction and remained relatively unchanged from 2 to 96 h, (between 497 and 521 mV). The addition of CC in ratios of 1:1 and 1:0.5 slightly decreased the Eh of the system, while a CPY:CC ratio 1:0.25 significantly reduced the Eh values to a range within 393–434 mV. The addition of BC in ratios of 1:1 and 1:0.5 of CPY:BC decreased the Eh, while their addition in a ratio of 1:0.25 slightly increased the Eh values compared to CPY's Eh values.

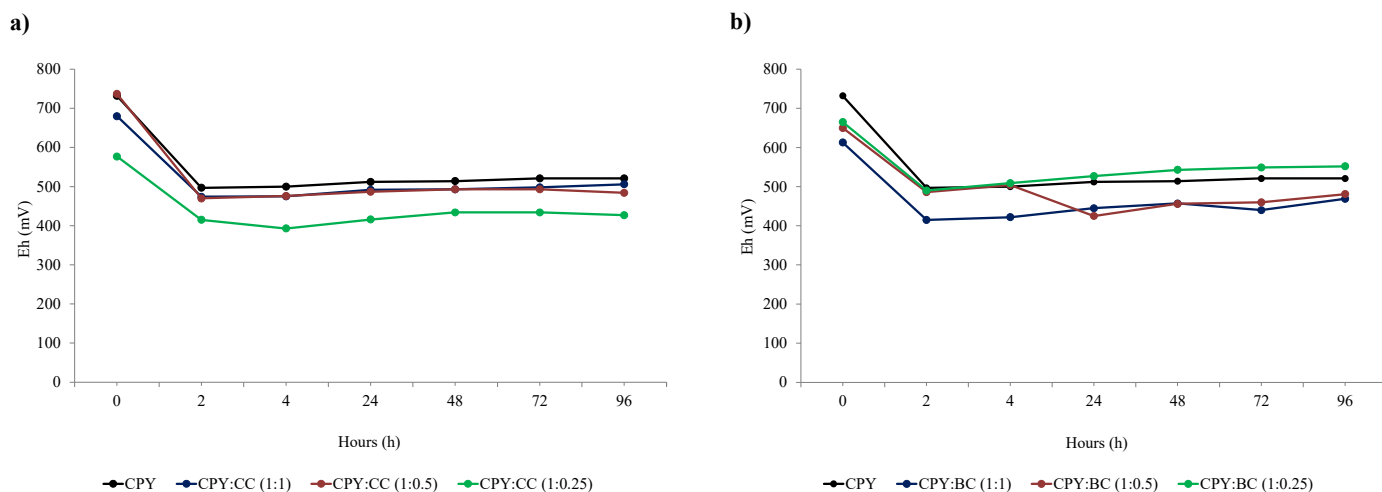


Figure 6. Eh (mV) evolution during leaching experiments with the addition of carbon materials: (a) CC and (b) BC.

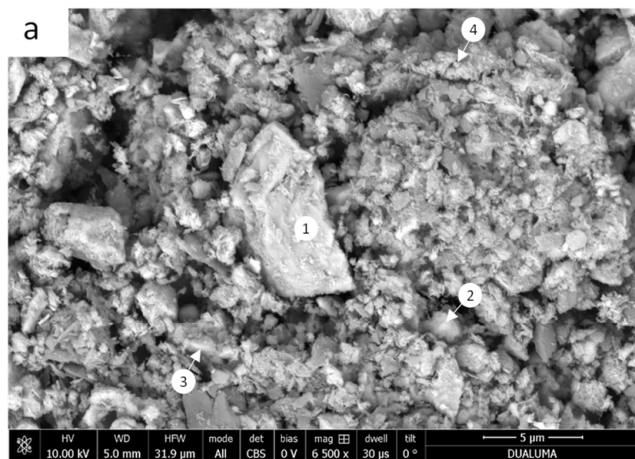
2.6. Solid Residue Analysis after Leaching Experiments

The characterization of solid residues obtained after CPY leaching with and without the addition of two carbon materials (CC and BC) at 1:1 and 1:0.25 ratios was performed by XRD (Table 4) and SEM-EDS (Figures 7 and 8).

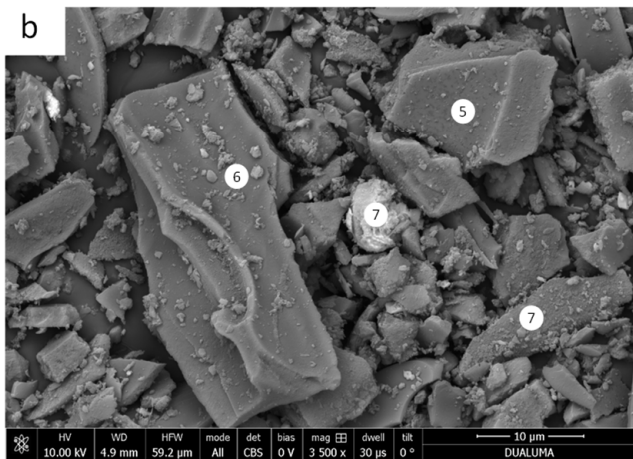
Table 4. XRD analysis of final solid residues after leaching process.

Final Solid Residue	Pyrite (%)	CuS (%)	Chalcopyrite (%)	Covellite (%)	Calcite (%)	Sulfur (%)	Jarosite (%)	Quartz (%)
CPY	35.0	—	54.0	8.0	0.6 *	2.0	—	1.0
CPY:CC 1:1	89.0	—	—	—	3.8	—	—	7.6
CPY:CC 1:0.25	47.7	51.8	—	—	0.4 *	—	—	0.1
CPY:BC 1:1	39.7	—	39.5	—	1.0	14.1	—	traces
CPY:BC 1:0.25	45.2	—	6.5	—	—	43.4	3.7	—

* For crystalline phases with a content of less than 1%, the quantification is approximate.

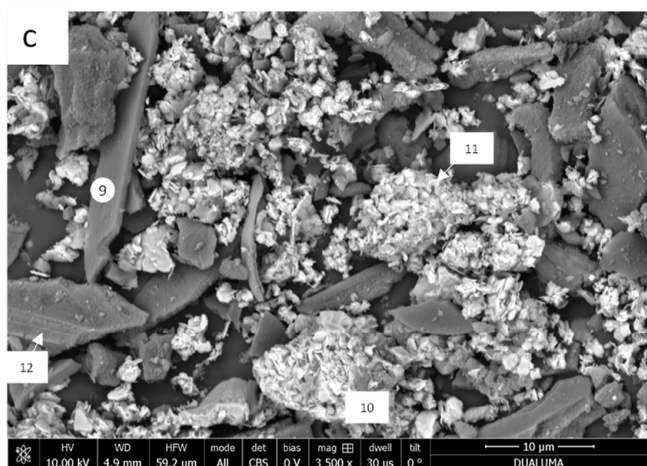


Point	Atomic content (%)				
	S	Fe	Cu	O	Si
1	42.04	25.02	32.94		
2	44.59	29.29	1.78	23.15	1.19
3	41.71	29.97		25.42	2.90
4	4.45	29.22	1.83	58.90	5.60

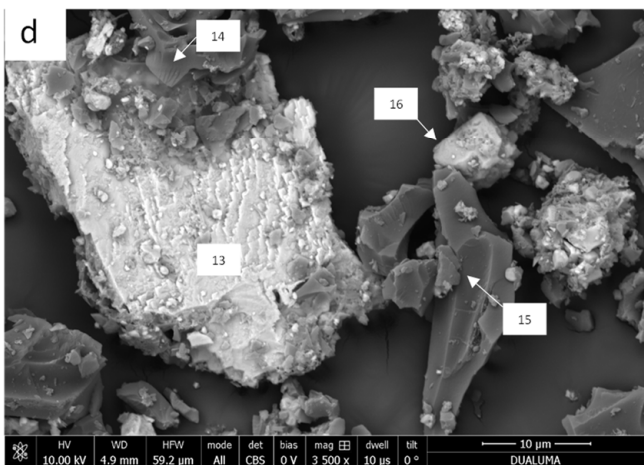


Point	Atomic content (%)					
	C	S	Fe	Cu	O	Si
5	79.89	15.43	2.12		2.55	
6	88.41	6.36	0.46		4.77	
7	85.15	5.98	1.93		6.89	0.06
8		62.29	37.71			

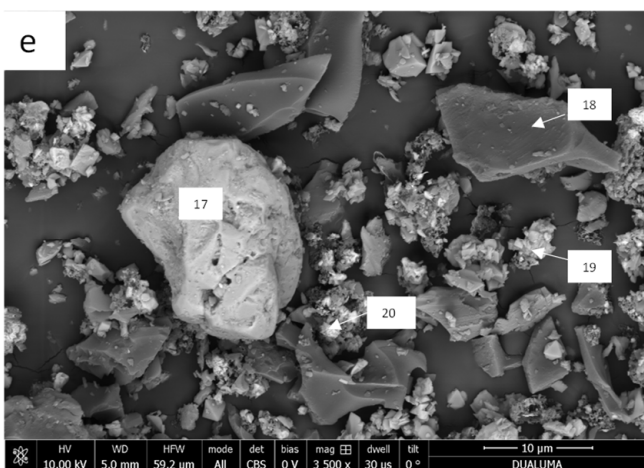
Figure 7. Cont.



Point	Atomic content (%)					
	C	S	Fe	Cu	O	Si
9	88.54	2.71	0.26	1.42	6.14	0.93
10	35.97	27.52		36.27		0.24
11	61.89	16.23		18.57	2.80	0.51
12	83.67	5.49	1.01	2.30	7.29	0.24



Point	Atomic content (%)					
	C	S	Fe	Cu	O	Si
13	35.04	27.32	15.61	19.13	2.91	
14	97.27	0.21			2.52	
15	91.34	0.35			8.31	
16	69.24	12.10	6.44	2.54	9.25	0.43



Point	Atomic content (%)					
	C	S	Fe	Cu	O	Si
17		62.28	37.72			
18	83.47	1.99	0.41	0.19	13.72	0.22
19	51.27	20.52	13.76		13.21	1.24
20	65.61	12.93	16.26		4.67	0.53

Figure 7. SEM-EDS images of final residues obtained after 96 h of leaching: (a) CPY; (b) CPY:CC 1:1; (c) CPY:CC 1:0.25; (d) (CPY:BC 1:1); (e) (CPY:BC 1:0.25).

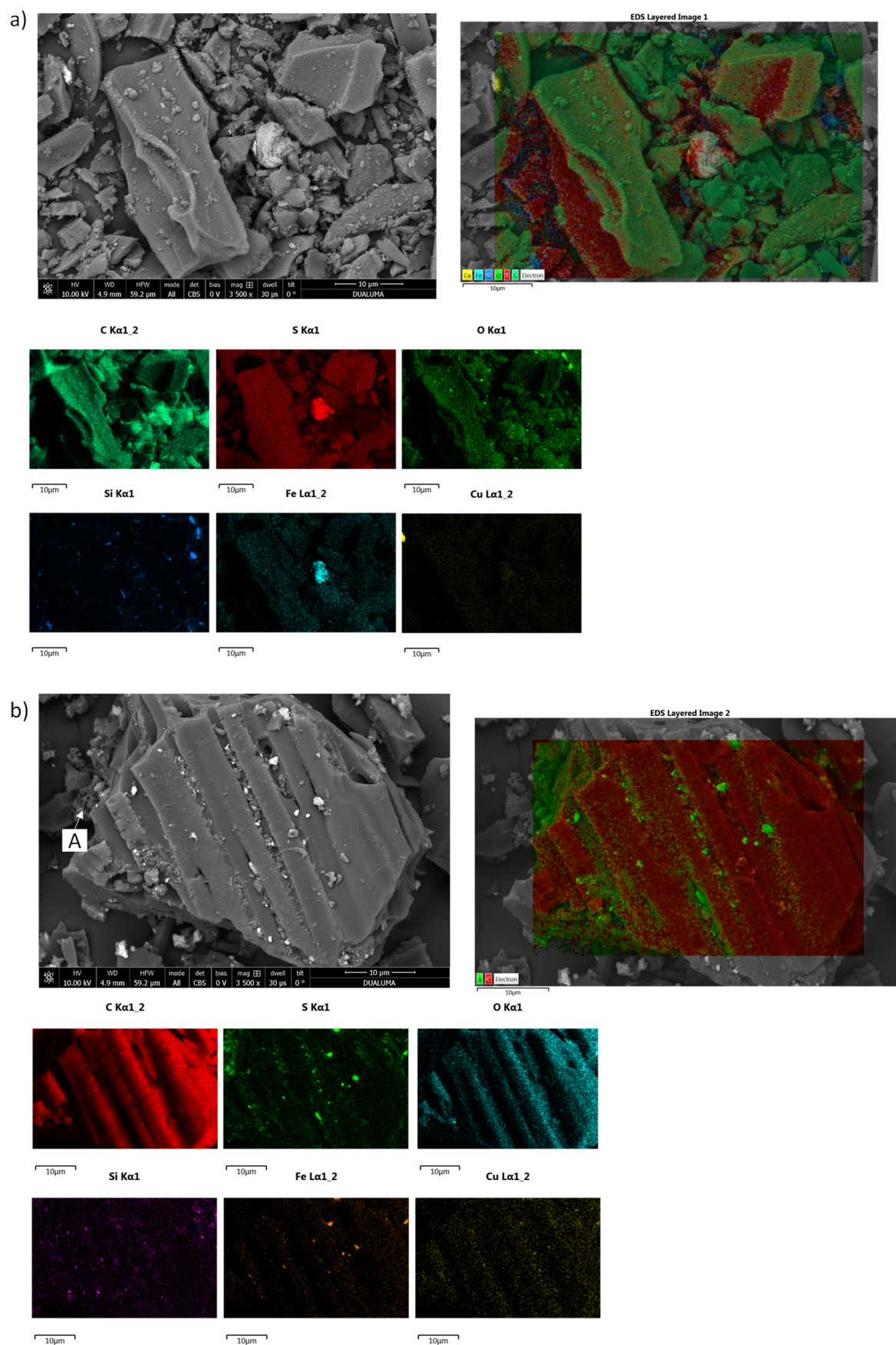


Figure 8. SEM-EDS images of CC (a) and BC (b). A: elemental sulfur.

The solid residue of CPY leaching showed the presence of pyrite (35%) and chalcopyrite (54%) with small amounts of covellite (8%), sulfur (2%), quartz (1%), and calcite (0.6%). However, the solid residue of the CPY:CC in the 1:1 ratio was mainly composed of pyrite (89%) and small amounts of quartz (7.6%) and calcite (3.8%). The presence of copper minerals was not observed due to the high extraction of Cu (99.1%). Interestingly, the high CuS content (51.8%) and the absence of chalcopyrite were observed in the solid residue of the leaching system of the CPY:CC of ratio 1:0.25.

The addition of BC leads to a final residue with characteristics different from those obtained in the presence of CC. With BC, large amounts of sulfur were observed (43% in the CPY:BC ratio of 1:0.25) that probably were produced during the first steps of the leaching process due to the low presence of oxygenated groups on the BC surface. Furthermore, jarosite formation (7%) was observed for the CPY:BC ratio of 1:0.25. This occurrence was based on the high Eh values of the extractant, favoring the formation of jarosite (Figure 6b).

Figure 7 shows SEM-EDS images of the final residues and corroborates the results obtained by XRD. Figure 7a shows SEM images of the solid residue after leaching of CPY. The presence of large chalcopyrite particles can be observed (point 1), with small particles of pyrite with different oxidized minerals (points 2, 3, and 4). Images of the solid residue after leaching of the sample CPY:CC 1:1 (Figure 7b) show the presence of activated carbon with sulfur atoms on its surface and some Fe (points 5, 6, and 7) and pyrite (point 8). The presence of copper was not observed, in agreement with its high extraction value (99.1%). Figure 7c shows images of the solid residue obtained after leaching of the sample CPY:CC 1:0.25. The presence of sulfur and copper can be observed on the surface of CC, probably due to CuS (points 9–12). The analysis of solid residues after leaching of CPY with BC is shown in Figure 7d (CPY:BC ratio 1:1) and 6.e (CPY:BC ratio 1:0.25). According to the XRD analysis (Table 4), there are chalcopyrite particles (point 13) similar to the solid residue of leaching of CPY without biochar. Compared to CC addition, BC particles showed a low amount of sulfur on their surface (points 14 and 15), indicating a low biochar adsorption capacity consistent with the lower surface area of BC. Some sulfur present on the BC surface could be due to a reaction with a leaching agent (Table 4) and the low adsorption of sulfur species. Finally, aggregates of different minerals were observed (point 16). Concerning solid residues in the CPY:BC ratio 1:0.25, the presence of pyrite (point 17); BC combined with small amounts of S, Cu, and Fe (point 18); and mixtures of small particles of different minerals and carbon particles (points 19 and 20) can be observed.

Figure 8 shows SEM-EDS images of CC and BC after leaching experiments. In the case of CC, the sulfur was evenly distributed on the entire surface of the CC particles (Figure 8a). In the case of BC, the amount of sulfur adsorbed was lower, and a large part of the sulfur was combined with iron. In addition, the formation of elemental sulfur can be observed (point A). Finally, it is important to note that a large amount of iron was found on the surface of the CC, while in the case of BC, the iron content on the BC surface was lower.

3. Discussion

Previous work has shown that the presence of functional groups, especially hydroxyquinone and quinone groups, greatly influences the catalytic properties of carbon materials during oxidative leaching of sulfide minerals, allowing for reversible redox reactions [27]. Hammes et al. [28] concluded that materials with highly condensed aromatic carbon rings have H/C ratios lower than 0.3, as is the case for CC. The O/C ratio of CC (0.11) was higher than that of BC (0.01), showing the presence of more oxygen functionalization in CC, related to such functional groups' generation during activation processes of commercial activated carbons. Oxygen can appear on carbon surfaces in different functional groups, such as hydroxyl, carbonyl, carboxyl, or ester groups. The concentration of different functional groups and the oxygen availability can influence the catalytic properties of carbon materials. The addition of two carbon materials (CC and BC), despite their different properties, can increase copper extraction from chalcopyrite. The effectiveness of the extraction process depends on the properties of the carbon material and their proportion in the leaching

system. In fact, it is possible to reach Cu extraction values of 91.1% (CPY:BC ratio 1:0.25) and of 99.1% (CPY:CC ratio 1:1). The percentages were higher than that obtained previously in the leaching of a complex sulfide mineral (52.6% chalcopyrite, 32.2% sphalerite, and 8.4% pyrite) [25], indicating the influence of mineral composition on the addition of carbon materials and their proportion in the leaching system.

Figure 4 shows that there was an important increase in copper extraction for the CPY:CC ratio 1:1 (after 48 h of leaching) and for the CPY:BC 1:0.25 ratio (after 72 h of leaching). These results could indicate the formation of intermediate species during the first hours of extraction that are more amenable to oxidation. Previous works have concluded that copper extraction is mainly controlled by: (1) the redox potential of the leaching solution, (2) the concentration of ferric/ferrous ions, and (3) the formation of intermediate species that are oxidized in a lower potential region with higher ferrous concentrations that enhance copper extraction [29]. Furthermore, it can be proposed that the surface of a carbon material can be modified by a sulfuric/ Fe^{3+} solution, increasing its content in oxygen functional groups and modifying its catalytic effect over time [27]. For this reason, characterization of BC and CC was performed after treatment of carbon materials for 48 h with the leaching agent at 90 °C. Treatment with sulfuric/ Fe^{3+} solution modified the characteristics of CC and BC (Table 2 and Figure 5). It is important to note that the ash content decreased, particularly in BC, indicating the solubilization of the ash components.

For this reason, in the future use of carbon materials as catalysts in these leaching conditions, it will be of interest to prepare materials with a low ash content to avoid additional contamination of the leaching liquors. A significant increase in the O content of BC was observed, indicating the generation of oxygenated groups on the biochar. The sulfuric/ Fe^{3+} solution treatment also increased the S content and decreased the H/C ratio, probably due to the oxidation of more aromatic structures and the formation of –OH and –COOH groups. This result indicates that the BC sample can achieve catalytic properties during treatment with sulfuric/ Fe^{3+} acid due to the in-situ formation of active groups, in agreement with the increase in the recovery of copper from the CPY:CC 1:0.25 sample after 72 h of leaching (Figure 4b).

In conclusion, adding either material (BC or CC) can increase copper extraction despite their differences in surface area, functional groups, and Eh values (Table 2). This fact can be explained by the optimal ratios were different for each material, and biochar was oxidized during the leaching process with the formation of C=O and C-O groups such as quinones, carboxylic acids, ethers or esters, or phenolic groups. Nakazawa [23] observed an increment from 28 to 90% in the extraction of copper after adding carbon black (surface area: 65 m²/g, particle media diameter: 36 nm) to chalcopyrite during leaching with a sulfuric/ferric solution at 50 °C. Therefore, the surface area is not the only or main factor involved in the catalytic effect of carbon materials, as it is possible to use cheaper materials prepared without activation processes, such as the biochar used in the present research. Finally, it can be concluded that some copper is adsorbed onto the material's surface and recovered by washing with an acid solution at the end of the leaching process (see Table 3 and Figure 4). Nakazawa [23] used carbon black in sulfuric acid media at 50 °C and proposed that the enhanced leaching kinetics of chalcopyrite could be due to dissolution reactions at low redox potential joined to the galvanic interaction between carbon black structures and chalcopyrite. This author showed that the acceleration of chalcopyrite extraction did not occur without direct contact between particles of carbon black and chalcopyrite and that the addition of carbon black decreased the ferric/ferrous ratio in the early stages of extraction and lowered the redox potential below 600 mV. Other researchers [14,29] concluded that the redox potential is a key factor in the leaching of chalcopyrite and proposed a critical potential, suggesting that chalcopyrite dissolves through the formation of intermediate species. Cordoba et al. proposed that a high potential for extraction favors rapid precipitation of ferric materials such as jarosite and the corresponding passivation of chalcopyrite [14]. Also, Hiroyoshi et al. noted that the redox potential must be low enough for Cu_2S formation and high enough for its subsequent oxidation [29]. This fact can explain

the behavior of the treatment of the CPY:BC ratio 1:0.25. Briefly, Eh decreased during the first 4 h, increasing later from 509 to 552 mV. However, although the amount of copper extracted was higher for the CPY:CC ratio 1:1, Eh was similar during the leaching time. For each carbon material (CC or BC), the highest values of copper extraction were achieved when the ratio between the carbon material and the solution yielded the highest value of Eh. It can be concluded that factors such as galvanic interactions contribute to the catalytic effect of carbon. The final catalytic effect was a consequence of different physicochemical processes making an optimal ratio depending on the characteristics of carbon materials. In order to achieve a better understanding of the carbon material's effect on copper extraction from chalcopyrite, the final residues were widely characterized.

The presence of CuS in the final residue of CPY:CC ratio 1:0.25 indicates that the addition of CC and the reduction of Eh modified the reaction mechanism, which was performed via intermediate CuS formation. Finally, the addition of CC at both ratios (1:1 and 1:0.25) seems to inhibit the formation of elemental sulfur. Lemos et al. [30] found that activated carbons promote the oxidation of aqueous sulfide to form polysulfides, especially disulfide, and oxygenated sulfur species such as sulfite, sulfate, and thiosulfate but not elemental sulfur. Additionally, they concluded that this oxidation increases when the activated carbon contains oxygen groups on its surface, such as quinone/hydroquinone and carboxylic acids.

The presence of pyrite (89%) and small amounts of quartz (7.6%) and calcite (3.8%) as the unique mineralogical species in the final residue of extraction of CPY:CC ratio 1:1 (Table 4) is of great importance for the future industrial implementation of processes based on the addition of activated carbon. This fact can limit the environmental impact of mine waste, as pyrite could be recovered from the waste by flotation processes. It is known that the oxidation of pyrite in mine ponds is responsible for the formation of acidic waters. Finally, it is interesting to note the presence of calcite after leaching of samples in acidic media. Its presence is higher in samples with CC and BC, probably due to their presence in its ashes. Previous works have shown that gypsum can precipitate on the surface of dissolving calcite in acidic media if the solutions have high sulfate concentrations and low pHs [31,32]. These coatings on the calcite's surface can reduce contact between the solution and calcite, leading to decreased dissolution rates.

An interesting result is the influence of the carbon material on the elemental sulfur content. Similar results have been obtained previously using biomass-derived activated carbon as an additive in the leaching of sulfide minerals [33]. The sulfur adsorption onto the carbon materials was higher for CC than for BC. This fact may play an important role in the leaching mechanism of chalcopyrite and other sulfide minerals, inhibiting the formation of a sulfur passivation layer on the surface of the mineral. Though BC does not adsorb sulfur, its addition to CPY in low ratios also increases the copper extraction, indicating that, galvanic interactions were probably the main factor influencing the catalytic effect of the carbon material. However, other characteristics of carbon materials, such as their capacity to adsorb sulfur and their promotion of sulfide oxidation, could have contributed to this positive effect on the total copper extraction. The presence of CC can inhibit the formation of elemental sulfur (Table 4) due to its adsorption and probable combination with functional groups on the surface of CC. The surface area of BC was lower than that of CC (Figure 2); this fact could explain the differences observed in sulfur adsorption capacity between BC and CC. Jahromi and Ghahreman [26] have shown that some carbon materials adsorb elemental sulfur onto their surfaces, facilitating the potential to remove sulfur from the leaching residue.

4. Materials and Methods

4.1. Samples Selection and Characterization

A chalcopyrite ore sample (CPY) was obtained from a copper sulfide deposit located in the Huelva region (Spain). CPY was air-dried and sieved below 50 μm using a Retsch RM 100 mortar mill. (Retsch-Verder Scientific, Haan, Germany) The pH and redox potential

(Eh) of CPY were determined with a CPY/distilled water ratio of 1:2.5. The pH was measured using a Crison micro pH 2000 ((Crison, Barcelona, Spain)), and the Eh (mV) was measured using a pH 60 DHS ((XS Instruments. Capry, Italy). Wavelength X-ray fluorescence (WDXRF) was performed SCAY-Malaga University in an ARL ADVANT XP + sequential model from THERMO (Thermo Fisher Scientific, Waltham, MA, EEUU). Concentration data were obtained using the UNIQUANT integrated software ((Thermo Fisher Scientific, Waltham, EEUU). XRD was performed using a Bruker model D8 Advance A25 diffractometer (Bruker corporation, Billerica, MA, EEUU).

Two carbon materials, a commercial activated carbon (CC) supplied by Panreac (Barcelona, Spain) and commercial biochar (BC), were selected for this research [25,34]. The BC sample was air-dried, crushed, and sieved (<100 μm) using a ceramic mortar. The two samples, BC and CC, were characterized according to BET surface (SBET) ($\text{m}^2 \text{g}^{-1}$), pore volume ($\text{cm}^3 \text{g}^{-1}$), ash content (wt%), and elemental analysis (C, H, N, O, and S%). SBET was analyzed by N_2 adsorption isotherms using an ASAP 2420 Porosimetry System by Micromeritics (Micromeritics, Dunstable, England). Elemental analysis was determined using a LECO CHNS 932 Analyzer (LECO corporation, St. Joseph, MI, EEUU) by dry combustion. The ash content was calculated by the combustion of samples in a Labsys Setaram TGA analyzer ((KEP Technologies, Mougins, France); 20 mg of each sample were heated at a rate of $15 \text{ }^\circ\text{C min}^{-1}$ to $850 \text{ }^\circ\text{C}$ using 30 mL min^{-1} of air. Oxygen was obtained by difference as $100\% - (\%C + \%H + \%N + \%S + \%Ash)$. Atomic ratios of H/C and O/C were calculated from the elemental analysis results. In addition, FTIR analysis was performed in a Vertex 70 spectrophotometer ((Vertex, Barcelona, Spain). For the acquisition of spectra, a standard spectral resolution of 4 cm^{-1} was used in the spectral range of $4000\text{--}400 \text{ cm}^{-1}$, with 64 accumulations per sample.

4.2. Leaching Experiments

The leaching agent was a sulfuric acid solution with 5 g L^{-1} of Fe (III). The purities of the sulfuric acid and Fe (III) sulfate hydrated supplied by Panreac (Barcelona, Spain) were 97% and 99.5%, respectively. In each experiment, approximately 5 g of CPY samples was mixed with 100 mL of leaching agent solution and added to a 500 mL glass flask. The CPY:carbon material ratios (weight:weight) were 1:1, 1:0.5, and 1:0.25, except for the control. The glass flask was introduced into a heating mantle with magnetic stirring (Nahita Serie 658, Auxiliab, Navarra, Spain; heating power of 250 W) and temperature control inside the glass flask. Experiments were carried out at $90 \text{ }^\circ\text{C}$ with a stirring speed of 250 rpm. At different times (2, 4, 24, 48, 72, and 96 h), 1 mL of the supernatant solution of each leaching experiment was withdrawn. To achieve that, the stirring was stopped at each time to let the sample stand and favor its decantation. One mL of the supernatant solution was removed, filtered, and transferred to a 25 mL graduated flask, and the rest of the flask was filled with distilled water. To maintain the same system conditions, 1 mL of the leaching agent solution was added after each extraction. Copper extraction from CPY was calculated as shown in Equation (1):

$$\text{Cu extraction (\%)} = (\text{Cu content in leaching solution (g)}/\text{Cu content in CPY(g)} \times 100 \quad (1)$$

After 96 h, the stirring was stopped. When the samples reached room temperature, the pulp was filtered, and the solid residue was washed three times with 50 mL of H_2SO_4 solution at $\text{pH} = 2$ to recover the potential copper adsorbed onto the surface of the CC or BC. Total copper extraction was determined considering the copper content after leaching for 96 h and the copper content in the washed solutions. Copper was measured using an AAnalyst 400 PerkinElmer (AAS) spectrometer (Perkin Elmer, Waltham, MA, EEUU). The Eh of the leaching system was determined at different reaction times (0, 2, 4, 24, 48, 72, and 96 h) using a potentiometer of the model 60 DHS XS with an Ag/Ag+ electrode, and values were converted to the standard hydrogen electrode (SHE).

Leaching experiments and determination of Eh, pH, and copper extraction were performed in triplicate.

Furthermore, CC and BC were put in contact for 48 h with the leaching agent (without the CPY) at 90 °C in order to assess the interaction between the leaching agent and the carbon materials. This provided information about possible modifications to carbonaceous structures.

4.3. Characterization of Solid Residue

The final solid residue obtained after leaching of CPY with a sulfuric/ferric solution was analyzed by XRD (see Section 2.1). In addition, SEM-EDS analysis was performed using a Helios Nanolab 650 dual beam microscope from FEI Company with a Schottky field emission source for SEM (FESEM) and a Tomahawk focused ion beam (FIB) (FEI company, Hillsboro, OR, EEUU). The microscope was equipped with an energy-dispersive X-ray detector (EDS) and an electron-backscatter diffraction detector (EBSD) from Oxford Company (Oxford Lab products, Waples, San Diego, CA, EEUU). CC and BC after treatment with the leaching agent were characterized by FTIR, ash content, and elemental analysis.

5. Conclusions

The main conclusions of the present research are the following:

Commercial activated carbon or biochar in the appropriate ratio, despite their different properties, can increase the extraction of copper during sulfuric/ferric oxidation of chalcopyrite. Despite the general reduction of Eh in the presence of carbon, for each carbon material, the highest copper extraction is achieved in the mixture that gives the highest value of Eh.

Commercial activated carbon and biochar were oxidized during treatment with sulfuric/ferric solution, and biochar probably displayed catalytic properties in the leaching medium.

The final residue of chalcopyrite leaching in the presence of activated carbon with a ratio of 1:1 is mainly composed of pyrite and quartz with sulfur compounds on the surface of activated carbon particles. This result is of great importance in the future industrial implementation of this hydrometallurgical process for the treatment of chalcopyrite, as it can increase the extraction of copper and facilitate the recovery of pyrite and sulfur from the solid residue.

The carbon catalysts used are cost-effective and can be synthesized in a carbon-negative manner. Our research demonstrates how to recover copper from a refractory mineral, reducing the environmental impact of mine wastes while achieving a carbon offset.

Author Contributions: A.A.B., G.G., J.P.-F. and A.M. conceived the experiment, collected and analyzed the data, and wrote the article. All authors have read and agreed to the published version of the manuscript.

Funding: This research has been funded by the Ministerio de Ciencia, Innovación y Universidades (MCIU), Agencia Estatal de Investigación (AEI), and Fondo Europeo de Desarrollo Regional (FEDER) with grant number RTI2018-096695-B-C31.

Data Availability Statement: The data that support the findings of this study are available from the corresponding author (A. Méndez), upon reasonable request.

Conflicts of Interest: The authors declare no conflict of interest.

References

1. Lovik, A.N.; Hagelüken, C.; Patrick Wäger, P. Improving supply security of critical metals: Current developments and research in the EU. *SM&T* **2018**, *15*, 9–18. [[CrossRef](#)]
2. Ciacci, L.; Fishman, T.; Elshkaki, A.; Graedel, T.E.; Vassura, I.; Passarini, F. Exploring future copper demand, recycling and associated greenhouse gas emissions in the EU-28. *Global Environ. Chang.* **2020**, *63*, 102093. [[CrossRef](#)]
3. Nguyen, R.T.; Eggert, R.G.; Mike, H.; Severson, M.H.; Corby, G.; Anderson, C.G. Global Electrification of vehicles and intertwined material supply chains of cobalt, copper and nickel. *Resour. Conserv. Recycl.* **2021**, *167*, 105198. [[CrossRef](#)]
4. Arendt, R.; Bach, V.; Finkbeiner, M. Environmental costs of abiotic resource demand for the EU's low-carbon development. *Resour. Conserv. Recycl.* **2022**, *180*, 106057. [[CrossRef](#)]
5. Norgate, T.; Jahanshahi, S. Low grade ores-smelt, leach or concentrate? *Miner. Eng.* **2020**, *23*, 65–73. [[CrossRef](#)]

6. Wang, S. Copper leaching from chalcopyrite concentrates. *JOM* **2002**, *57*, 48–51. [[CrossRef](#)]
7. Watling, H.R. Chalcopyrite hydrometallurgy at atmospheric pressure: 1. Review of acidic sulfate, sulfate–chloride and sulfate–nitrate process options. *Hydrometallurgy* **2012**, *140*, 163–180. [[CrossRef](#)]
8. Dutrizac, J.E. Elemental sulphur formation during the ferric sulphate leaching of chalcopyrite. *Can. Metall. Q.* **1989**, *28*, 337–344. [[CrossRef](#)]
9. Majima, H.; Awakura, Y.; Hirato, T.; Tanaka, T. The leaching of chalcopyrite in ferric chloride and ferric sulfate solutions. *Can. Metall. Q.* **1985**, *24*, 283–291. [[CrossRef](#)]
10. McMillan, R.S.; Mackinnon, D.J.; Dutrizac, J.E. Anodic dissolution of n-type and p-type chalcopyrite. *J. Appl. Electrochem.* **1982**, *12*, 743–757. [[CrossRef](#)]
11. Muñoz, P.B.; Miller, J.D.; Wadsworth, M.E. Reaction mechanism for acid sulfate leaching of chalcopyrite. *Metall. Trans. B* **1979**, *10*, 149–158. [[CrossRef](#)]
12. Ammou-Chokroum, M.; Cambazoglu, M.; Steinmetz, D. Oxydation menagée de la chalcopyrite en solution acide: Analyses cinétique de réactions. II. Modèles diffusionales. *Bull. Miner.* **1977**, *100*, 161–177. [[CrossRef](#)]
13. Hackl, R.P.; Dreisinger, D.B.; Peters, E.; King, J.A. Passivation of chalcopyrite during oxidative leaching in sulfate media. *Hydrometallurgy* **1995**, *39*, 25–48. [[CrossRef](#)]
14. Córdoba, E.M.; Muñoz, J.A.; Blázquez, M.L.; González, F.; Ballester, A. Leaching of chalcopyrite with ferric ion. Part II: Effect of redox potential. *Hydrometallurgy* **2008**, *93*, 88–96. [[CrossRef](#)]
15. Pinches, A.; Al-Jaid, F.O.; Williams, D.J.A. Leaching of chalcopyrite concentrates with thiobacillus ferrooxidans in batch culture. *Hydrometallurgy* **1976**, *2*, 87–103. [[CrossRef](#)]
16. Watling, H.R. The bioleaching of sulphide minerals with emphasis on copper sulphides—a review. *Hydrometallurgy* **2006**, *84*, 81–108. [[CrossRef](#)]
17. Koleini, S.M.J.; Aghazadeh, V.; Sandstrom, A. Acidic sulphate leaching of chalcopyrite concentrates in presence of pyrite. *Miner. Eng.* **2011**, *24*, 381–386. [[CrossRef](#)]
18. Mehta, A.P.; Murr, L.E. Fundamental studies of the contribution of galvanic interaction to acid-bacterial leaching of mixed metal sulphides. *Hydrometallurgy* **1993**, *9*, 235–256. [[CrossRef](#)]
19. Zhong, S.; Li, Y. An improved understanding of chalcopyrite leaching kinetics and mechanisms in the presence of NaCl. *J. Mater. Res. Technol.* **2019**, *8*, 3487–3494. [[CrossRef](#)]
20. Nakazawa, H.; Nakamura, S.; Odashima, S.; Hareyama, W. Effect of carbon black to facilitate galvanic leaching of copper from chalcopyrite in the presence of manganese (IV) oxide. *Hydrometallurgy* **2016**, *163*, 69–76. [[CrossRef](#)]
21. Toro, N.; Pérez, K.; Saldaña, M.; Jeldres, R.I.; Jeldres, M.; Cánovas, M. Dissolution of pure chalcopyrite with manganese nodules and waste water. *J. Mater. Res. Technol.* **2020**, *9*, 798–804. [[CrossRef](#)]
22. Misra, M.; Fuerstenau, M.C. Chalcopyrite leaching at moderate temperature and ambient pressure in the presence of nanosize silica. *Miner. Eng.* **2005**, *18*, 293–297. [[CrossRef](#)]
23. Nakazawa, H. Effect of carbon black on chalcopyrite leaching in sulfuric acid media at 50 °C. *Hydrometallurgy* **2018**, *177*, 100–108. [[CrossRef](#)]
24. Okamoto, H.; Nakayama, R.; Kuroiwa, S.; Hiroyoshi, N.; Tsunekawa, M. Catalytic effect of activated carbon and coal on chalcopyrite leaching in sulfuric acid solutions. *Shigen-to-Sozai* **2004**, *120*, 600–606. [[CrossRef](#)]
25. Álvarez, M.L.; Fidalgo, J.M.; Gascó, G.; Méndez, A. Hydrometallurgical recovery of Cu and Zn from a complex sulfide mineral by Fe³⁺/H₂SO₄ leaching in the presence of carbon-based materials. *Metals* **2021**, *11*, 286. [[CrossRef](#)]
26. Nazari, G.; Dixon, D.G.; Dreisinger, D.B. Enhancing the kinetics of chalcopyrite leaching in the Galvanox™ process. *Hydrometallurgy* **2011**, *205*, 251–258. [[CrossRef](#)]
27. Jahromi, F.G.; Ghahreman, A. Effects of surface modification with different acids on the functional groups of AFS catalyst and its catalytic effect on the atmospheric leaching of enargite. *Colloids Interfaces* **2019**, *3*, 45. [[CrossRef](#)]
28. Hammes, K.; Smernik, R.J.; Skjemstad, J.O.; Herzog, A.; Vogt, U.F.; Schmidt, M.W.I. Synthesis and characterisation of laboratory charred grass straw (*Oryza sativa*) and chestnut wood (*Castanea sativa*) as reference materials for black carbon quantification. *Org. Geochem.* **2006**, *37*, 1629–1633. [[CrossRef](#)]
29. Hiroyoshi, N.; Miki, H.; Hirajima, T.; Tsunekawa, M. A model for ferrous-promoted chalcopyrite leaching. *Hydrometallurgy* **2000**, *57*, 31–38. [[CrossRef](#)]
30. Lemos, B.R.S.; Ivo, F.; Teixeira, I.F.; Mesquita, J.P.; Ribeiro, R.R.; Donnici, L.C.; Lago, R.M. Use of modified activated carbon for the oxidation of aqueous sulfide. *Carbon* **2012**, *50*, 1386–1393. [[CrossRef](#)]
31. Huminicki, D.M.C.; Rimstidt, J.D. Neutralization of sulfuric acid solutions by calcite dissolution and the application to anoxic limestone drain design. *Appl. Geochem.* **2008**, *23*, 148–165. [[CrossRef](#)]
32. Fusi, L.; Primicerio, M.; Monti, A. A model for calcium carbonate neutralization in the presence of armoring. *Appl. Math. Model.* **2015**, *39*, 348–362. [[CrossRef](#)]
33. Méndez, A.; Álvarez, M.L.; Fidalgo, J.M.; Di Stasi, C.; Manyà, J.J.; Gascó, G. Biomass-derived activated carbon as catalyst in the leaching of metals from a copper sulfide concentrate. *Miner. Eng.* **2022**, *183*, 107594. [[CrossRef](#)]
34. Álvarez, M.L.; Méndez, A.; Rodríguez-Pacheco, R.; Paz-Ferreiro, J.; Gascó, G. Recovery of zinc and copper from mine tailings by acid leaching solutions combined with carbon-based materials. *Appl. Sci.* **2021**, *11*, 5166. [[CrossRef](#)]